International Journal of Fluid Machinery and Systems
Vol. 8, No. 3, July-September 2015

DOI: 10.5293/IJFMS.2015.8.3.183
ISSN (Online): 1882-9554

Original Paper

Comparative study of sediment erosion on alternative designs of Francis runner blade

Bidhan Rajkarnikar[1], Dr. Hari P. Neopane[2] and Biraj S. Thapa[3]

[1]Department of Mechanical Engineering, Kathmandu University
Dhulikhel, Nepal, bidhan.rajkarnikar@gmail.com
[2]Department of Mechanical Engineering, Kathmandu University
Dhulikhel, Nepal, hari@ku.edu.np
[3]Department of Mechanical Engineering, Kathmandu University
Dhulikhel, Nepal, bst@ku.edu.np

Abstract

The aim of this study was comparative analysis of sediment-induced erosion on optimized design and traditional design of Francis runner blade. The analysis was conducted through laboratory experiments in a test rig called Rotating Disc Apparatus. The results showed that the extent of erosion was significantly less in the optimized design when compared based on the material loss. It was observed that the optimized design could reduce sediment erosion by about 14.4% if it was used in place of the reference design for entire duration of the experiment. Based on the observations and results obtained, it has been concluded that the optimization of hydraulic design of blade profile of Francis runner can significantly reduce the effect of sediment-induced erosion.

Keywords: Francis turbine; optimized design; rotating disc apparatus; runner blade; sediment erosion; wear pattern.

1. Introduction

1.1 Background

The erosion of turbine components due to effect of sediments in the river water is one of the major challenges in development of hydropower in Nepal. The rivers in this region contain high percentage of hard abrasive minerals like quartz, which causes rapid erosion of turbine components and affects the performance of turbines [1]. This in turn decreases the efficiency, reliability and operating life of the turbines and creates a serious challenge in operation of the hydropower project [2]. Although, sand traps and settling basins are installed in hydropower plants to filter out sands from the river water before introducing to turbines, the complete removal of sediments is not possible [1]. Very fine sand particles (less than 0.2 mm in diameter) are less likely to settle down in the settling basins and thus escape into the turbines. These sand particles are mainly responsible for the erosion in turbine components. The hydraulic turbines of several other Asian and South American hydropower projects are also facing this problem [1]. The problems of sediment erosion have also been reported in hydropower plants with comparatively lower sediment concentration as in Norway [2].

1.2 Current status of research

The study of sediment erosion in hydraulic turbines is very complex. Several attempts have been made to address the issue of sediment problems in hydro turbines. Major research works were mostly focused on establishing empirical relations to estimate the effects of sediment erosion in hydraulic turbines and identification of the parameters upon which the erosion rate is dependent. Various mathematical models have been developed to estimate the effect of sediment erosion in different hydraulic components of the power plant [2-11]. These mathematical models are generally empirical and statistical models developed from experimental measurements at the project site. Some studies have also been carried out to investigate the effect of size and concentration of silt particles on Pelton turbine buckets through laboratory experiments [8, 9]. Some of the earlier researches were focused on the impact of sediment particles on turbine materials [11-17], and to identify coating materials to protect the surface of the turbine components exposed to sediments [11-14]. Researches have also been carried out for complete mechanical design of turbines by selection of different erosion resistant materials and coatings [18, 19].

Recent researches [20-25] have shown a possibility to reduce the amount of sediment erosion in Francis turbines by reducing

Received Agust 7 2014; revised November 19 2014; accepted for publication August 25 2015: Review conducted by Professor Shogo Nakamura. (Paper number O14024J)
Corresponding author: Bidhan Rajkarnikar , bidhan.rajkarnikar@gmail.com

the relative velocity of water inside the runner, which is achieved by the optimization of the hydraulic design of turbine. The optimization process includes optimization of the runner blade profile to reduce sediment erosion, while avoiding cavitation and maintaining the highest possible efficiency. The hydraulic design parameters have been varied within a defined range to obtain less possible erosion in the runner. The optimization process has been carried out in a new design program named as "Khoj" which can generate the profiles of Francis runner based on the traditional equations. These optimized designs have further been analyzed with the help of numerical programming tools and Computational Fluid Dynamics (CFD) software to evaluate the hydraulic performance and erosion on blade surface of each design and comparisons have been made for the results of the optimized design with that of reference designs [20-25]. The results of these studies have revealed that the shape of runner blade has a significant effect on velocity distribution and hence on the sediment erosion of the runner. The results show that it is possible to reduce the sediment erosion in runner up to 33% by improvement in hydraulic design of turbine runner.

The present study intends to analyze the effect of sediment erosion in the reference as well as the optimized design through laboratory experiments. For this purpose, a test setup called Rotating Disc Apparatus (RDA) have been designed, developed and installed at the Turbine Testing Lab (TTL) in Kathmandu University of Nepal [26]. The major aim of this study is to compare the effects of erosion induced by river sediments on the reference and optimized designs of Francis runner blade and to verify if the optimized design is better than the reference design.

2. Experiment

2.1 Rotating Disc Apparatus

The sediment erosion testing of the Francis blades were done in the Rotating Disc Apparatus. The test apparatus uses sample rotation method in which the test sample is rotated in a mixture of calculated amount of sand and water. The 3D Computer Aided Design (CAD) model of the test rig is shown in Fig. 1 [26]. The detail features of the test setup have been described earlier by Rajkarnikar [26]. The RDA consists of an erosion chamber, inside which a disc consisting samples of turbine blades rotates. The rotating disc is attached to a shaft which is driven by a 3 phase 7.5 kW AC motor. The power from the motor is transferred to the shaft with the help of a V-belt drive with pulley ratio of 1:2.

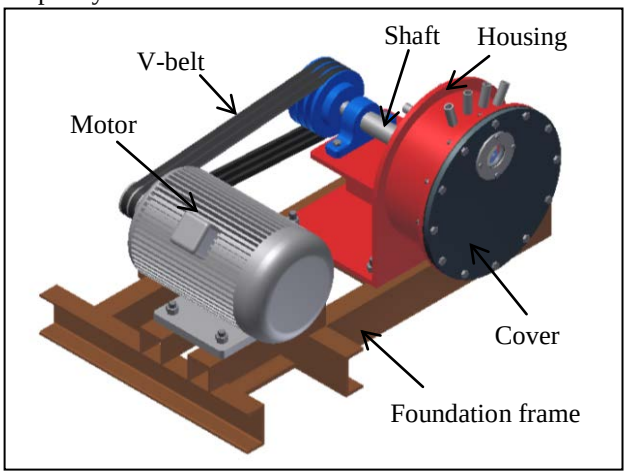

Fig. 1 3D CAD model of Rotating Disc Apparatus.

2.2 Test specimens

The test specimens used in this study were the models of Francis runner blade. Since the main objective of this study was to compare the performance of two different designs of Francis turbine runner, test specimens of both the runners have been fabricated. The two different designs of blades used were:

1) Reference design: The blade profile has been generated using traditional method of designing Francis runner.
2) Optimized design: The blade profile has been designed to reduce the effect of sediment erosion while producing same power under same basic operating condition as of the reference design.

The designs of blades have been used from earlier studies [20-25]. In these studies, the blades have been designed using the basic parameters of Jhimruk Hydroelectric Centre (JHC) (see Table 1). The optimized design of Francis runner has been developed by varying hydraulic design parameters of the reference design within a defined range to obtain less possible erosion maintaining same power output. The optimization process has been carried out in a program called 'Khoj'. CFD simulations have been carried out to evaluate the hydraulic performance and erosion on blade surface of each design and comparisons have been made for the results of the optimized design with that of reference designs [20-25].

Table 1 Basic design data for runner at JHC.

SN	Parameters	Value	Unit
1	Net design head, H	201.5	m
2	Design flow rate, Q	2.35	m3/s
3	Runner efficiency, η	96	%

The blade designs developed in those studies have been used in this study by scaling down to 1:4 ratio. This has been done to accommodate four numbers of blades in the rotating disc of 280 mm diameter. For fabrication of the model blades, both the designs were first modelled into 3D CAD models in Autodesk® Inventor®. The blades were modelled together with blade base for casting as a single block. The 3D CAD models were then printed into plastic models with the help of a 3D printer installed in

TTL. The plastic models were replicated into test specimens for using in the experiments by Wax lost casting method. In order to get measurable amount of wear in a short period, Aluminum with 6 % Copper and 4 % Zinc has been used as the material for test specimens instead of hard materials like turbine steels. The additional metals have been added to make the specimens slightly stronger than pure aluminum. Figure 2 shows the plastic model, the wax replica and the final aluminum test specimen of optimized design.

Fig. 2 (a) Plastic model, **(b)** the wax replica, **(c)** final aluminum test specimen of optimized design.

2.3 Experimental procedure

Since the main objective of the experiment was to compare the effect of sediments in two different designs, various parameters common for the test run were set to be constant throughout the experiment. The descriptions of these parameters are listed in Table 2.

Table 2 Parameters of laboratory setup.

Parameters	Value
Speed of rotation of motor	2880 rpm
Speed of rotation of disc	1440 rpm
Direction of rotation of disc	Clockwise as viewed from front
Diameter of disc	284 mm
Radius of mounting of specimen	100 mm
Volume of water in casing	6.17 liters
Specimens used	(a) Blade of reference design named as design A (b) Blade of optimized design named as design B
Material of specimen	Aluminum with 6 % Copper and 4 % Zinc for increasing strength
Number of specimen	A single set contains four numbers of blades: two each for both designs. The test specimens are named as A1, B2, A3 and B4.
Operating time	45 minutes
Total number of observations	8
Water	Used from the water supply of TTL
Sediment concentration	Since, the test being carried out needs to produce result in very less time as compared to the actual site condition, the rate of erosion should be accelerated with the help of higher concentration of sediment. Thus, the sand concentration is selected as 85,900 ppm, which requires 530 gm. of sand in a single run.
Sediment used	Sand sample of tailrace of Sunkoshi Hydropower Plant.
Sediment particle size	Size ranging from 0.125 to 0.2 mm.
Thermometer	Alcohol type, range -10 to 110°C
Pressure Gauge	Relative pressure gauge, range 0 to 20 kg/cm² ± 2%
Weight balance	Electronic weighing machine of Ohaus Corporation, USA Item no. E11140, max. 110 gm., least count 0.1 mg.

The test specimens were thoroughly cleaned with detergent solution, dried and weighed before each test runs. The internal surface of the casing, cover and inspection glass was also cleaned. The clean set of test specimens were mounted on the disc. Fig. 3 shows the mechanism of mounting test specimens on the disc. Each test specimen consisted of a blade and a circular plate called blade base. The test specimen was mounted in the disc with the help of the blade base. The disc had four circular seats where the blade base fitted perfectly as shown in Fig. 3. Each test specimen was attached to the disc with the help of countersunk screw and nut. The holes in the blade base for mounting screws had been drilled in such a way that the angle of relative velocity of water at the leading edge of the test specimen was 30°. In case of real turbines, this angle depends upon the opening of the guide vanes [27].

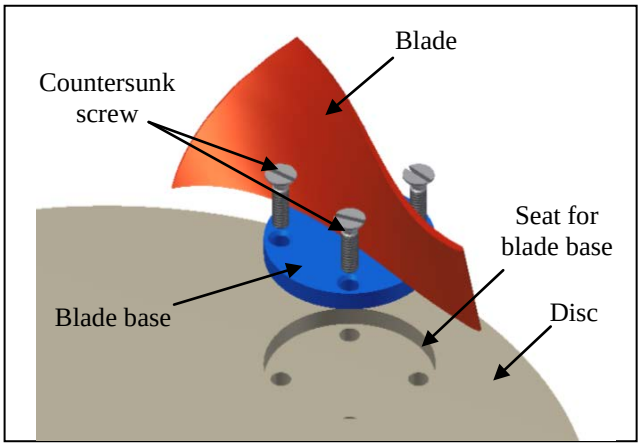

Fig. 3 The mounting procedure of test specimen on disc.

The disc was mounted on the shaft and tightened with the help of luck nut. After the cover of the housing was closed and the nut and bolts were tightened securely, the casing was filled with a mixture of sand and water at required concentration, and the test run was started. After running the apparatus for predefined period, the motor was stopped and the slurry mixture inside the casing was drained out by opening the drain plug. The disc was removed from the shaft; the test specimens were removed from the disc, and washed thoroughly with detergent and clean water. The weight loss measurements were taken with the help of the Electronic weighing machine as specified in the Table 2. The weight loss was calculated by noting down the difference between the weight of the test specimens before and after each test run. The photographs of the surface of specimens were also recorded to observe the pattern of wear being developed after each test run.

The patterns of erosion on the surface of test specimens were also observed with the help of painted surface. This was done to quickly identify the location of wear in the blade surface. The test specimens were spray painted to obtain smooth paint surface and dried for about 40 hours before the test. The specimens were then mounted on the disc and the apparatus was run for about half an hour to observe the removal of paint from the blade surface. The test pieces were taken out of the apparatus, cleaned and dried thoroughly. Photographs were taken and compared with the photographs taken prior to running the test.

3. Observations and discussion

3.1 Flow pattern around the blades

A CFD analysis was performed for simulation and analysis of the flow pattern around the rotating blades in the RDA. The CFD was carried out to ensure if the flow of water around the test specimens was similar to the flow of water in real turbine blades. A rotating domain shown in the Fig. 4(a) has been referred. The mesh for CFD was developed in ANSYS Mechanical, which constituted 689,368 nodes and 3,570,843 elements. The mesh structure is shown in Fig. 4(b). The flow streamline obtained from the analysis showed that water was flowing on the entire surface of the blades. Figure 4(c) shows the velocity streamline in the test blades obtained from the CFD analysis. Compared to the velocity streamline obtained from CFD analysis conducted by Shrestha [28] on a Francis turbine runner as shown in Fig. 4(d), the flow pattern is similar in the test specimen to that in real turbine runner. The velocity was low in the leading edge of the blades and gradually increased as the water flowed towards the trailing edge of the blade. The velocity was highest at the trailing edge, which is similar in case of a real turbine runner blade.

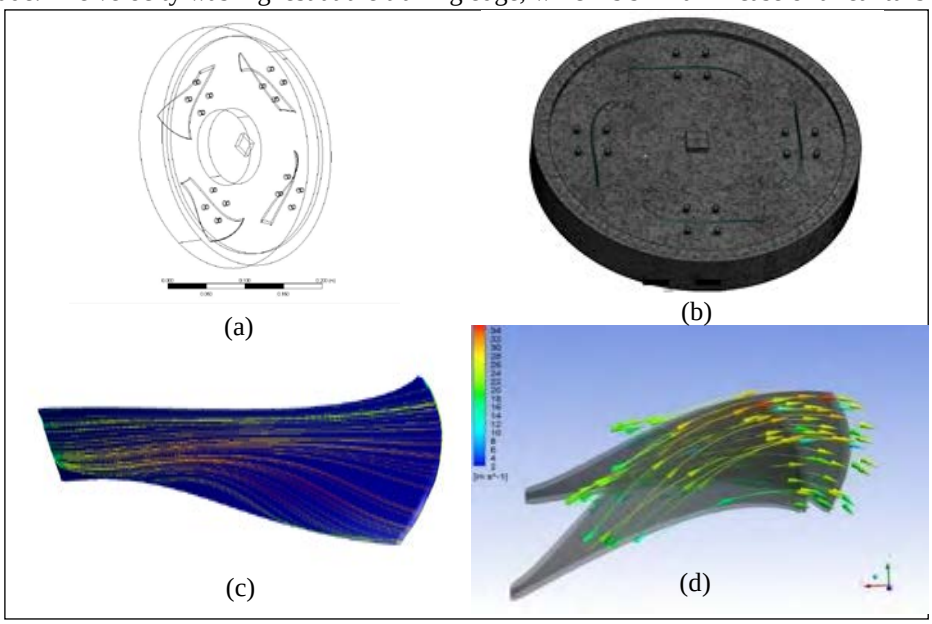

Fig. 4 CFD analysis. **(a)** Geometry of the rotating domain, **(b)** mesh structure, **(c)** velocity streamline on the test blades, **(d)** velocity streamline on a Francis runner blade [28].

3.2 Pattern of erosion

The paint of every test specimens was found to be removed. The locations of paint removal were observed to be similar in all the test specimens, mostly in the outlet region of the blade surface and in the inlet edge. Some minor scratches were also found throughout the blade surface. The removal of paint in the outlet region might have occurred due to micro erosion, which, according to Brekke [29], is caused due to high rotational motion of fine sand particles. Figure 5 shows the comparison of wear observed in the test specimens and the wear observed in the runner outlet of JHC [10]. It can be seen that the erosion damage is mostly located in the far outlet region near to the trailing edge of the blade, which is identical to the pattern of wear observed in the turbines operating in real cases. The relative velocity in the turbine is highest at the outlet of runner, close to the shroud. The high relative velocity causes high rotational motion of fine sand particles, which causes the micro erosion in this area. In addition, the runner outlet area is subject to cavitation wear if subject to low pressure. Thus, synergy between cavitation and sediment erosion can accelerate the wearing process considerably in this area.

Similarly, the removal of paint in the inlet edge might have occurred due to secondary flow vortex erosion. According to Brekke [29], this type of erosion generally occurs due to secondary flow caused by any obstacles in the flow path. The secondary flow occurring due to the obstruction caused by the leading edge of the test blade resulted into the erosion in this area. The erosion seen in this area of test blade is identical to the erosion occurring in real turbines as observed in the case of Cahua Power Plant, Peru [21] (Fig. 5).

Fig. 5 Wear observed in the test specimen and in the runner outlet of JHC [10] and inlet of Cahua Power Plant [21].

The observation of erosion pattern (see Fig. 6) further showed that the wear is concentrated in a small location in the optimized design while it is scattered along the blade surface of the reference design. Which indicated that the extent of wear is slightly less in the optimized design than in the reference design. The pattern of wear observed is also found to be nearly similar to the results of the CFD analysis of the two designs carried out in earlier studies [20-25] (see Fig. 6). It can be observed that in case of the reference design, the effect of sediment is in almost all of the area of the outlet region of blade, which is similar in the case of the result of CFD analysis. Meanwhile, comparatively small portion of the outlet region of the optimized blade has been affected by sediment, which is also nearly similar to the result of CFD analysis.

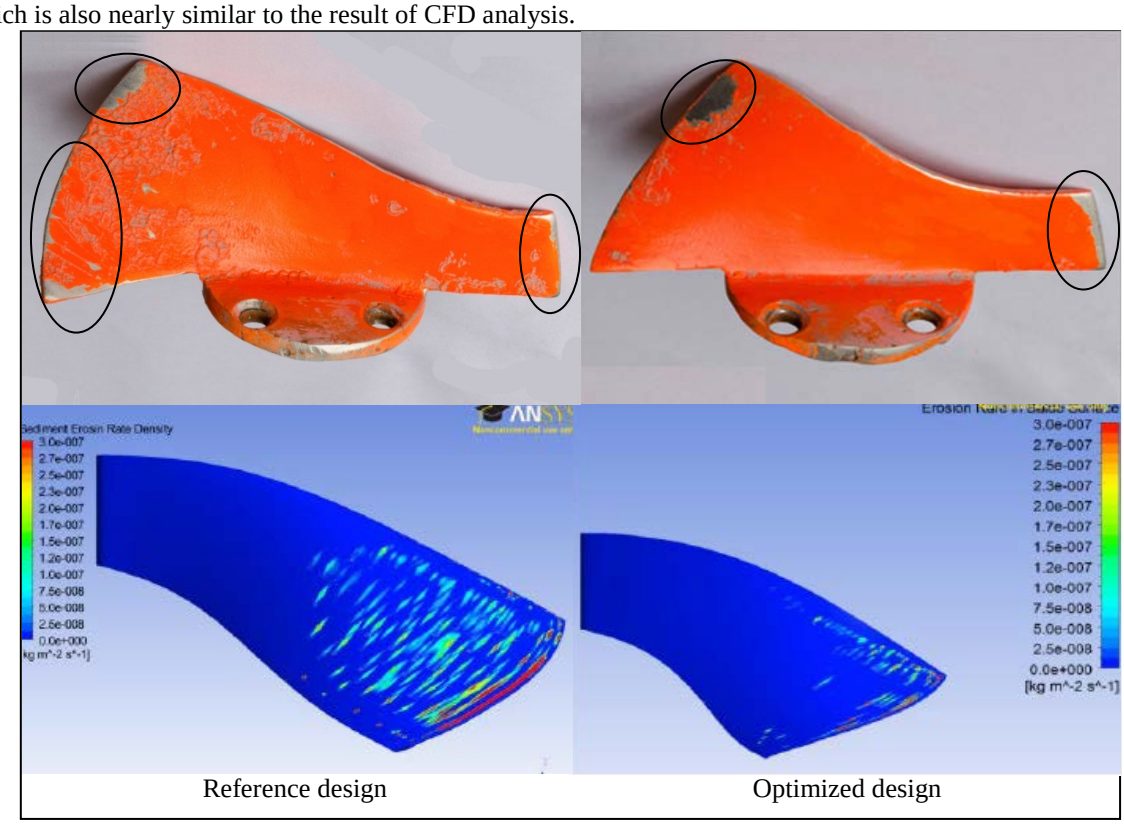

Fig. 6 Pattern of erosion observed in the test specimens and the results of CFD analysis [25].

The erosion was also observed in the suction side of the blades (see Fig. 7). The severity of erosion in the suction side has been observed equally in both the designs. The erosion is mostly observed in extreme outlet region of the blade close to shroud in both the designs. This indicates that though the optimized design is capable of reducing erosion in the pressure side of the blade, both the designs are almost equally affected by sediment in the suction side.

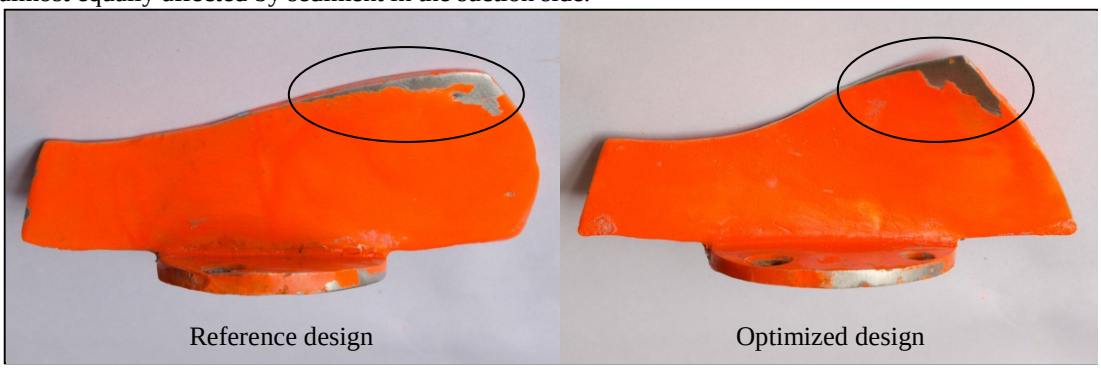

Fig 7 Wear observed in the suction side of test specimens.

The pattern of erosion was also investigated in the test runs carried out for observation of material loss. The tests were conducted on test specimens without paint. Photographs were recorded after every test run, some of which are shown in Fig. 8. The erosion pattern was developing gradually with increase in the operation time. Clear pattern of wear was observed after 125 minutes since cavitation erosion was also developing after this stage. The severity of damage was observed to be increasing after cavitation erosion was seen in the blades. This might have been caused due to combined effect of erosion and cavitation. The eroded surface might have further accelerated cavitation as well as erosion due to changes in the flow pattern of water through the damaged surface. It has also been observed that the erosion damage was severe in the spots having casting defects. This might have also occurred due to changes in the flow direction due to the defected surface. The photographs after 350 minutes further shows that the effect of erosion is slightly less in the optimized design than in the reference design. In the optimized design, wear is observed more in the inlet region of the blade rather than in the outlet region. While in the reference design, the effect of erosion is similar in the inlet and outlet region of the blade. Some traces of erosion are also seen in the midway of the reference design, which might have occurred due to the presence of casting defect in that location.

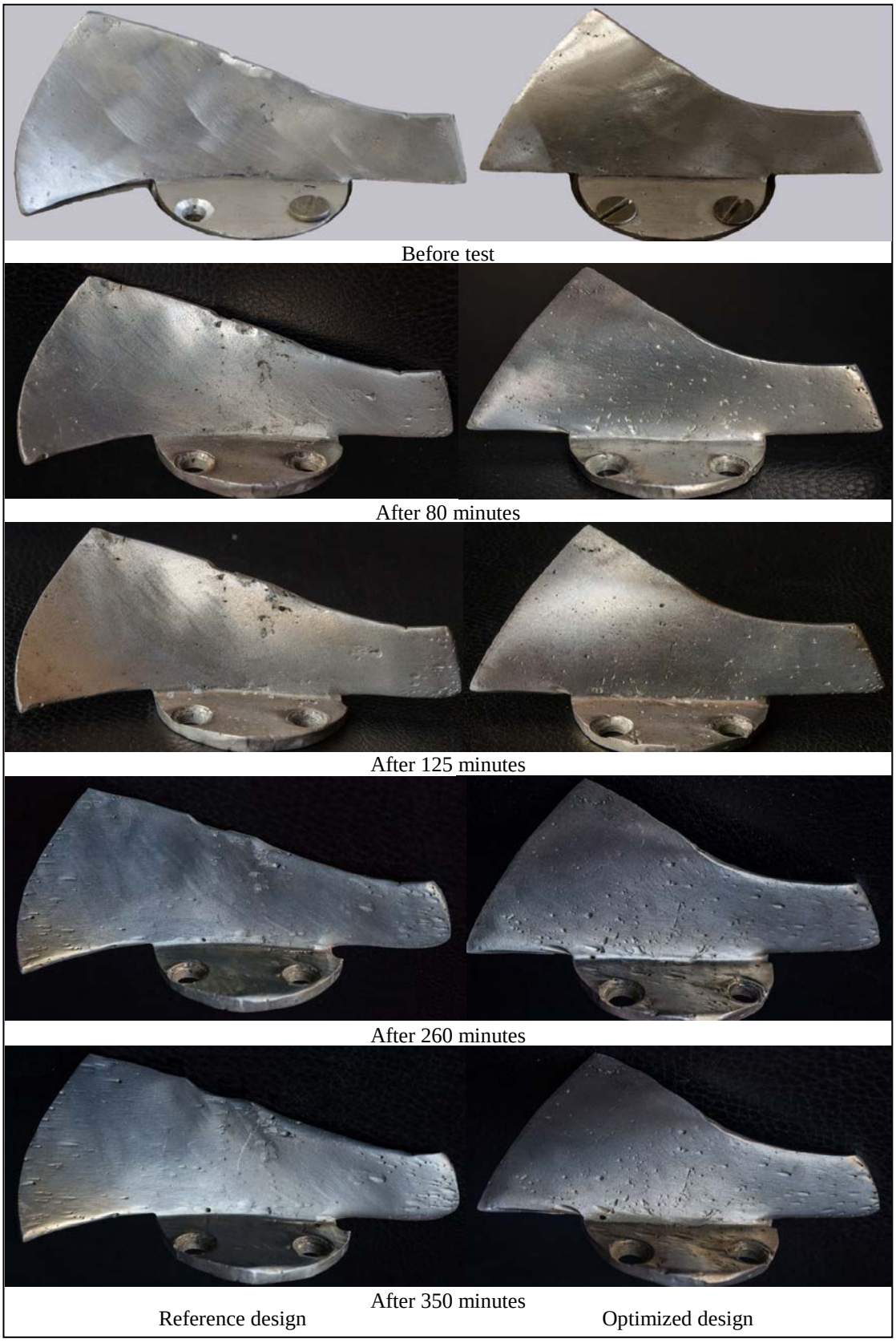

Fig. 8 Erosion in the test specimens during different stages of operation.

3.2 Loss of material

The recorded weights of all of the four test specimens are shown in Fig. 9(a) with respect to the duration of test run. The Fig. 9(a) shows that total weight loss in specimen A1 is higher than other three test pieces followed by specimen A3. The weight loss in optimized blades B2 and B4 are quite lesser than that in the reference blades A1 and A3. The higher value in A1 might have been obtained due to higher erosion caused by surface defects of casting.

For comparison of the two alternative designs of runner blade, the weights of the corresponding designs are summed up to obtain the combined weights of specimen A and B. Fig 9(b) shows the combined weights of the two alternative designs. It can be observed that the total loss in design A is higher than design B by more than 2 gm., which is a significant amount in case of such a

small test pieces. The graph also shows that the rate of decrease in the weight of design A is slightly higher than design B. This indicates that, if this rate of erosion continues for longer duration of operating time, the amount of weight loss in the reference design will be significantly higher than that in the optimized design.

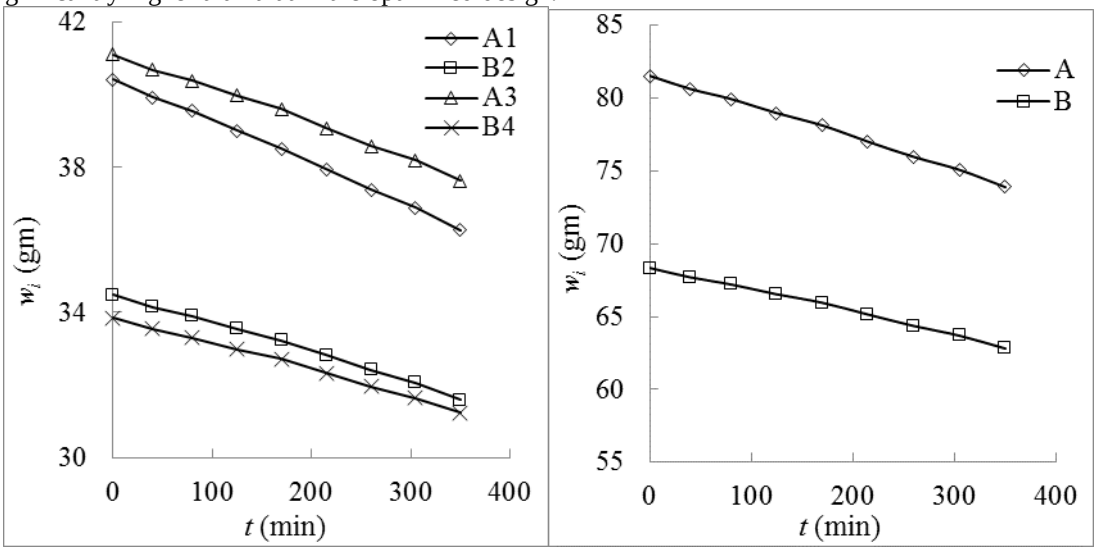

(a) (b)

Fig. 9 (a) Recorded weights of the test specimens after each test. **(b)** Combined weight of reference design and optimized design after each test.

The sand particle used in the experiment as erodent remain inside the system throughout a single test which is quite different from the real case where fresh sediment particles strike the blade surface continuously. As the introduced erodent keep striking the blade surface for entire duration of test, the erodent property is degraded due to particle degradation. The effect of this degradation has not been considered while calculating the amount of material loss in the test specimens, which suggests that the loss of material in the turbine of real cases is higher than that observed in this study.

The amount of erosion in the test specimens is analyzed in terms of cumulative erosion in both the designs. The cumulative erosion gives a picture of total erosion occurring in the specimens after each test run. It can also be defined as the ratio of total weight loss in the specimens from the beginning of the experiment to the original weight of the test pieces at the beginning, and expressed as weight loss in milligram per gram of test specimen. Equation (1) gives the cumulative erosion in the test pieces.

$$e_i = (w_0 - w_i)/w_0 \times 1000 \qquad [\text{mg/gm.}] \tag{1}$$

Figure 10 shows the graphical representation of the cumulative erosion in the test pieces. The total erosions in test specimens A and B after an operation of 350 minutes are 93.5 mg/gm. and 80.7 mg/gm. This indicates that during the entire experiment, 93.5 mg of material has been lost from 1 gm. of test specimen A. Similarly, 80.7 mg of material has been lost from 1 gm. of test specimen B due to sediment erosion. This further implies that the erosion in optimized design is considerably lesser than that in the reference design. The graph also shows that the amount of erosion is increasing with the time of exposure of test specimens to sediments. It is obvious, as the damaged surface of blades will further accelerate the erosion rate as it disturbs the flow of water. The difference between the lines is also increasing with time, which suggests that the erosion in reference design will keep on increasing in higher rate than in the optimized design.

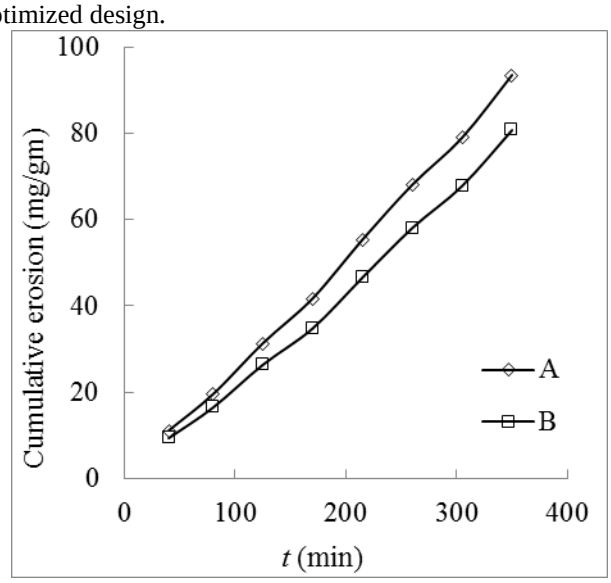

Fig. 10 Cumulative erosion in test specimens.

The difference in erosion has also been analyzed in terms of percentage difference, which is shown in Table 3. This quantity can be termed as the reduction in amount of erosion, which is achieved if the optimized design is used instead of the reference

design. The reduction in erosion is calculated using eq. (2).

$$\text{Reduction in erosion} = (e_A - e_B)/e_A \times 100 \quad [\%] \tag{2}$$

Table 3 Amount of reduction in erosion.

SN	Test duration (min)	Reduction in erosion (%)
1	40	14.76
2	80	15.94
3	125	16.55
4	170	19.31
5	215	14.33
6	260	10.63
7	305	11.69
8	350	12.16
	Average	14.42%

There is a significant amount of reduction in erosion in every test. However, no any clear trend has been observed in the reduction throughout the experiment. Thus, it is not possible to say about the reduction in erosion for longer operation time. The highest reduction in erosion has been recorded in test 4 with a value of 19.31% while, the least reduction in erosion is 10.63% in test 6. The average reduction throughout the experiment is 14.4%, which shows that the optimized design can reduce the erosion in average of 14.4% if used instead of the reference design.

3.3 Rate of Erosion

The rate of erosion can be defined as the amount of erosion per unit time of operation. The rate of erosion can be calculated using eq. (3).

$$\text{Rate of erosion} = (wi - wj)/(wi \times \Delta t) \times 1000 \quad [\text{mg/gm per min}] \tag{3}$$

Table 4 shows the rate of erosion in both the specimens for each test. It can be observed that the rate of erosion in specimen B is less than that in specimen A in all of the test runs. The average rate of erosion in specimen B is significantly lesser than that in specimen A which further justifies that the optimized design is less affected by erodent than the reference design. It can also be observed that the overall trend of the erosion rate for both test specimens is increasing with the total duration of the test run. This also implies that the rate of erosion is going to increase with increase in the time of exposure to erosion.

Table 4 Rate of erosion.

SN	Test duration (min)	Reduction in erosion (mg/gm. per min)	
		A	B
1	40	0.26	0.24
2	80	0.21	0.18
3	125	0.27	0.22
4	170	0.24	0.19
5	215	0.32	0.27
6	260	0.30	0.27
7	305	0.26	0.23
8	350	0.35	0.31
	Average	0.28	0.24

4. Conclusion

Based on the observations and results obtained from comparative study, it can be concluded that the optimized design is better than the reference design in handling sediment erosion. The extent of sediment-induced erosion was found to be significantly less in the optimized design when the comparison was made based on material loss. After an operation time of 350 minutes, the average rate of erosion in the reference design was 0.28 mg/gm. per min. While, the erosion rate in the optimized design was only 0.24 mg/gm. per min. It was also observed that the optimized design could reduce sediment erosion by about 14.4% if it has been used in place of the reference design for the entire duration of the experiment. The results also suggests that for longer operation time, the amount of erosion in the reference design keeps increasing with higher rate than in the optimized design. Thus, it can be concluded that the optimization of hydraulic design of blade profile of Francis runner can significantly reduce the effect of sediment-induced erosion.

Acknowledgments

The authors are grateful to EnPe-MPPOES programme and the Renewable Nepal programme for providing necessary fund to carry out this research. They are also thankful to the researchers and staffs of Turbine Testing Laboratory, Kathmandu University who have helped during experimentation and CFD analysis.

Nomenclature

e_A	Erosion in test specimen A [mg/gm.]	wi	Weight of test specimen before test [gm.]
e_B	Erosion in test specimen B [mg/gm.]	wj	Weight of test specimen after test [gm.]
e_i	Cumulative erosion after test i [mg/gm.]	Δt	Duration of test [min]
w_0	Weight of test specimen at the beginning of the experiment [gm.]		

References

[1] Thapa, B., Shrestha, R., Dhakal, P., Thapa, B.S. (2004). Sediment in Nepalese hydropower projects.
[2] Neopane, H. (2010). Sediment Erosion in Hydro Turbines. PhD Thesis at NTNU, Trondheim, Norway.
[3] Thapa, B. (2004). Sand Erosion in Hydraulic Machinery. PhD thesis at NTNU, Trondheim, Norway.
[4] Truscott, G.F. (1972). A Literature Survey on Abrasive Wear in Hydraulic Machinery. Wear. Volume 20, Issue 1, 29-50.
[5] Karelin, V.Y., Denisov, A.I., Yulin, Wu. (2002). Calculation of Hydraulic Abrasion. In: Duan CG and Karelin VY (eds.), Abrasive Erosion and Corrosion of Hydraulic Machinery. 53-94. Imperial College Press, London.
[6] Bajracharya, T.R., Acharya, B., Joshi, C.B., Saini, R.P., Dahlhaug, O.G. (2008). Sand erosion of Pelton turbine nozzles and buckets: a case study of Chilime hydropower plant. Wear. Volume 264, Issues 3–4, 177-184.
[7] Kurosawa, S., Nakamura, K., Wei, P. (2011). Sand Erosion Prediction for Hydraulic Turbine Runner. Proc. The 11th Asian International Conference on Fluid Machinery, IIT Madras, Chennai, India.
[8] Padhy, M.K., Saini, R.P. (2009). Effect of Size and Concentration of Silt Particles on Erosion of Pelton Turbine Buckets. Energy 34, 1477-1483.
[9] Bajracharya, T.R., Sapkota, D., Thapa, R., Poudel, S., Joshi, C.B., Saini, R.P., Dahlhaug, O.G. (2006). Correlation Study on Sand Led Erosion of Buckets and Efficiency Losses in High Head Power Plants. Proc. First National Conference on Renewable Energy Technology for Rural Development, Kathmandu, Nepal.
[10] Thapa, B.S., Thapa, B., Dahlhaug, O.G. (2012). Empirical modelling of sediment erosion in Francis turbines. Energy 41, 386-391.
[11] Wood, R.J.K. (1999). The sand erosion performance of coatings. Materials and Design 20, 179-191.
[12] Goyal, D.K., Singh, H., Kumar, H., Sahni, V. (2012). Slurry erosion behavior of HVOF sprayed WC–10Co–4Cr and Al2O3+13TiO2 coatings on a turbine steel. Wear 289, 46–57.
[13] Thapa, B., Upadhyay, P., Dahlhaug, O.G., Basnet, R., Timsina, M. (2005). HVOF coatings for erosion resistance of hydraulic turbines: Experience of Kaligandaki "A" Hydropower Plant. Water Resources and Renewable Energy Development in Asia.
[14] Padhy, M.K., Saini, R.P. (2008). A review on silt erosion in hydro turbines. Renewable and Sustainable Energy Reviews. 12, 1974–1987.
[15] Poudel, L., Thapa, B., Shrestha, B.P., Shrestha, N.K. (2012). Sediment Impact on Turbine Material: Case Study of Modi River, Nepal. Kathmandu University Journal of Science, Engineering and Technology. Vol. 8, No. I, 88-96.
[16] Matsumura, M., Chen, B.E. (2002). Erosion-Resistant Materials. In: Duan CG and Karelin VY (eds.), Abrasive Erosion and Corrosion of Hydraulic Machinery, 235-313, Imperial College Press, London.
[17] Chauhan, A.K., Goel, D.B., Prakash, S. (2008). Erosion behaviour of hydro turbine steels. Bull. Mater. Sci. Vol. 31, No. 2, 115–120, Indian Academy of Sciences.
[18] Erichsen, H.P. (2011). Mechanical design of Francis Turbine Exposed to Sediment Erosion. Master's Thesis at NTNU, Norway.
[19] Paulsen, J.B. (2011). FSI-analysis of a Francis turbine. Master's Thesis at NTNU, Norway.
[20] Thapa, B.S. (2011). Hydraulic Design of Francis Turbine to Minimize Sediment Erosion. Master's thesis at Kathmandu University, Nepal.
[21] Gjøsæter, K. (2011). Hydraulic design of Francis Turbine Exposed to Sediment Erosion. Master's Thesis at NTNU, Norway.
[22] Thapa, B.S., Eltvik, M., Gjøsæter, K., Dahlhaug, O.G., Thapa, B. (2012). Design Optimization of Francis Runners for Sediment Handling. Proc. of Fourth Int. Conf. on Water Resources and Renewable Energy Development in Asia, Thailand.
[23] Thapa, B.S., Panthee, A., Thapa, B. (2012). Computational Methods in Research of Hydraulic Turbines Operating In Challenging Environments. International Journal of Advanced Renewable Energy Research. Vol. 1, Issue 2, 95-98.
[24] Eltvik, M., Thapa, B.S., Dahlhaug, O.G., Gjøsæter, K. (2012). Numerical analysis of effect of design parameters and sediment erosion on a Francis runner. Int. J. Hydropower & Dams, Chiang Mai, Thailand.
[25] Thapa, B.S., Thapa, B., Dahlhaug, O.G. (2012). Current research in hydraulic turbines for handling sediments. Energy 47. Issue 1, 62-69.
[26] Rajkarnikar, B. (2013). Study of Sediment Erosion in Francis Turbine Runner at Laboratory Conditions. Master's Thesis at Kathmandu University. Lambert Academic Publishing, Germany. (ISBN: 978-3-659-38165-2)
[27] Brekke, H. (2002). Hydraulic Turbines Design, Erection and Operation. NTNU Publication.
[28] Shrestha, K.P., Thapa, B., Dahlhaug, O.G., Neopane, H.P., Thapa, B.S. (2012). Innovative Design of Francis Turbine for Sediment Laden Water. Proc. of TIM International Conference, Kathmandu, Nepal.
[29] Brekke, H. (2002). Design of Hydraulic Machinery Working in Sand Laden Water. In: Duan CG and Karelin VY (eds.), Abrasive Erosion and Corrosion of Hydraulic Machinery. 155-181. Imperial College press, London.